Site NGHP-01-08

By T. Collett, M. Riedel, J. Cochran, R. Boswell, J. Presley, P. Kumar, A. Sathe,
A. Sethi, M. Lall, and the National Gas Hydrate Program Expedition 01 Scientists

Scientific Investigations Report 2012–5054

U.S. Department of the Interior
U.S. Geological Survey

Contents

Figures

Site NGHP-01-08

By T. Collett, M. Riedel, J. Cochran, R. Boswell, J. Presley, P. Kumar, A. Sathe, A. Sethi, M. Lall, and the National Gas Hydrate Program Expedition 01 Scientists

Background and Objectives

Site NGHP-01-08 (Prospectus Site MNGH01-1-A) is located at 18° 57.4271' N, 085° 43.7393' E in the central part of the Mahanadi Basin (fig. 1). The water depth is ~1,689 m. The site is located within the Reliance Industry Ltd. D10 block with full 3D seismic coverage. Operations at this site are restricted to a total depth of 350 mbsf. This site was not selected as a primary coring site after the LWD/MWD campaign was completed.

The objectives of the work carried out at this site follow the general objectives of the India NGHP Expedition 01, but focus on the LWD/MWD operations only:

- Study the occurrence of gas hydrate and establish the background geophysical baselines for gas-hydrate studies;
- Define the relationship between the sedimentology and structure of the sediments and the occurrence and concentration of gas hydrate;
- Calibrate remote sensing data such as seismic data by acquiring LWD/MWD data;

The seismic data provided for this site (inline 2148) were extracted from the 3D cube (figs. 2 and 3). The seafloor deepens to the southeast along the line with a general slope of less than one degree. The seismostratigraphy is characterized by three distinctly different packages of sediments. The top ~100 mbsf is characterized by low-amplitude, constant-frequency reflections suggesting a series of thinly bedded layers. Below this sequence, a layer approximately 25 m thick can be identified, which lacks internal seismic reflectivity. Below this sequence the sediment layers show signs of minor deformation and non-confirmable contacts. The sequence extends to well below 350 mbsf (TD of Hole NGHP-01-08A). A strong BSR can be seen along the entire seismic line. The BSR occurs within the third package of sediments as described above at a depth of ~257 mbsf. The layers below the BSR occasionally show increased amplitudes likely due to gas changing.

Hole NGHP-01-08A targets a distinct reflection within the gas hydrate stability field at a depth of ~190 mbsf (2.463 s TWT). This reflection has relatively higher amplitudes than the surrounding sediments.

Operations

This operations summary covers the transit from Site NGHP-01-07 (KGGH06-A) to Site NGHP-01-08 (MNGH01-1-A) and LWD/MWD drilling operations in Hole NGHP-01-08A (fig. 4). Schedule details and statistics for this site can be found as Appendixes:

- Appendix 1: NGHP Expedition 01 Operations Schedules
- Appendix 2: NGHP Expedition 01 Operations Statistics

Included in the "Methods" chapter and the glossary is a list of standard or commonly used operations terms and acronyms.

Hole NGHP-01-08A

The 227.0 NMI transit from Site NGHP-01-07 to Site NGHP-01-08 was completed in less than a day at an average speed of 9.8 kt.

The first and only hole of Site NGHP-01-08 was drilled on Leg 2 of NGHP Expedition 01 as the eighth hole of a 12-hole LWD/MWD transect. The sea voyage ended at 1054 hr May 29, 2006; thrusters/hydrophones were immediately lowered. The vessel was switched from cruise mode to DP control at 1100 hr and at 1136 hr a positioning beacon was deployed at the Hole NGHP-01-08A location coordinates. The LWD/MWD tools, consisting of the GeoVISION (RAB), EcoScope, SonicVISION, and TeleScope, were assembled. After replacing batteries in the GeoVISION and SonicVISION tools a flow test was conducted identifying a problem with the SonicVISION tool. Less than one hour of troubleshooting led to a decision to replace the SonicVISION tool with the spare tool. The flow test was repeated and the nuclear source loaded. The drill string was subsequently lowered to the seafloor and the drill string was spaced out for spudding. A tag of the seafloor indicated a mudline depth of 1,700.0 mbrf. For reference, the PDR depth at this site, adjusted to the rig floor DES, was 1,701.4 mbrf. After offsetting the vessel 2 meters N of the site coordinates, Hole NGHP-01-08A was spudded at 2110 hr on May 29. LWD/MWD drilling continued at a controlled rate of 24.1 m/h (or 19.2 m/h average net ROP including connection time) to a total depth of 350.0 mbsf. The hole was displaced with 110 barrels of 10.5 ppg mud, the top drive was set back, and the drill string was pulled clear of the seafloor at 1655 hr May 30, 2006. After removing the nuclear source and downloading data, the LWD/

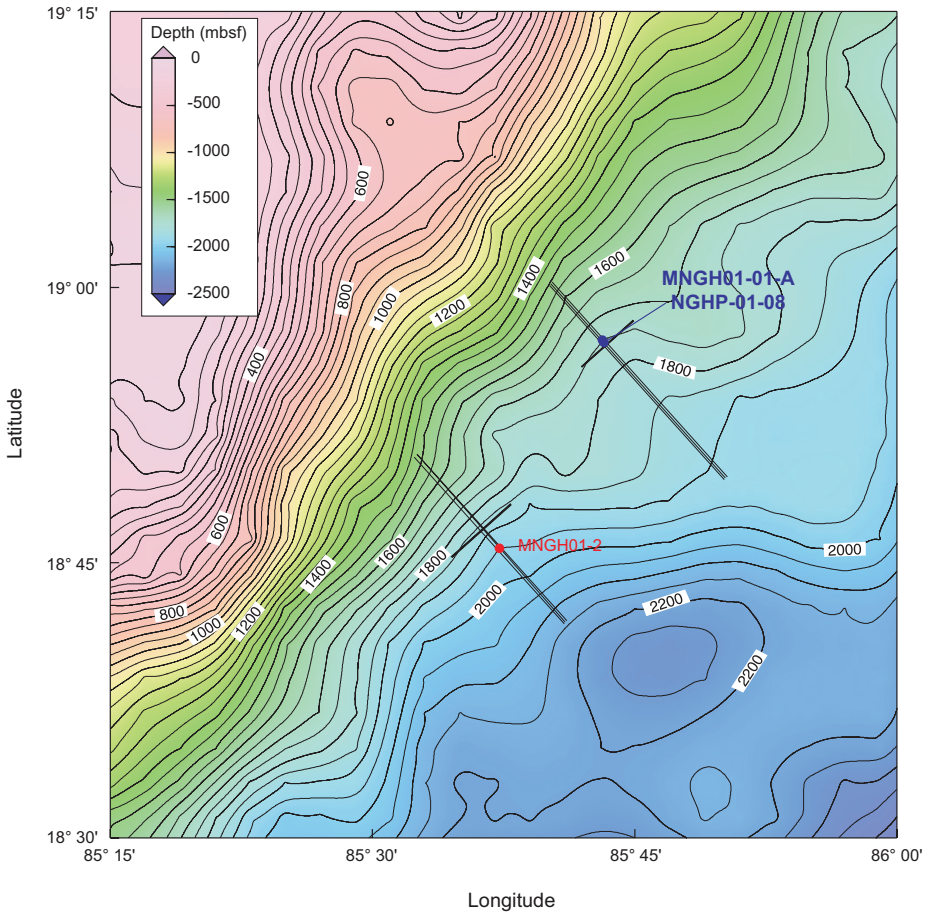

Figure 1. Location of Site NGHP-01-08 (Prospectus Site MNGH01-1-A) in the Mahanadi Basin.

MWD BHA was racked back in the derrick. The rig was secured for transit, the beacon recovered, and the vessel got underway for Site NGHP-01-09 (MNGH01-2) at 2118 hr. This completed operations at Site NGHP-01-08.

Downhole Logging

Logging While Drilling

Operations

After tagging the seafloor at 1,700 mbrf (driller's depth), Hole NGHP-1-08A was spudded at 2110 hr on May 29, 2006. LWD tools in the BHA included the GeoVISION, the EcoScope, the SonicVISION, and the TeleScope MWD. For details on each LWD tool and measurement, see the "Downhole Logging" section in the "Methods" chapter.

To avoid washing out the formation near the seafloor, Hole NGHP-01-08A was spudded at a relatively low flow rate. The first 10 m were drilled at 100 gallons per minute (gpm) with a rotation rate of 20 rotations per minute (rpm) and a rate of penetration (ROP) of 25 m/h. Below 10 mbsf, the rotation rate was increased to 30 rpm; at 30 mbsf, the rotation rate was increased to 60 rpm and the flow rate was increased until the LWD tools turned on (~370 gpm), while keeping a ROP of 25 m/h. The target depth of 350 mbsf (2,050 mbrf) was reached at 1522 hr on May 30, 2006. After pulling the drill string to the surface, data download and rig down were completed at 2030 hr on May 30. (The depths in mbsf mentioned above are referenced to the seafloor depth tagged by the driller.)

Gas Monitoring with Real Time LWD/MWD Data

The LWD logs were acquired at Hole NGHP-01-08A to plan possible coring and pressure-coring operations in subsequent holes. As Hole NGHP-1-08A was drilled without coring, the LWD data had to be monitored for safety to detect gas entering the wellbore. As explained in the "Downhole Logging" section of the "Methods" chapter, the primary measurement used for gas monitoring was the "annular pressure while drilling" (APWD) measured by the EcoScope tool in the borehole annulus. We looked for sudden decreases of more than 100 psi in the annular pressure, which could be due to low-density gas entering the wellbore. We also monitored pressure increases of the same magnitude, which could be due to fluid acceleration caused by a gas kick (Aldred and others, 1998).

Figure 5 shows the measured borehole fluid pressure profile in Hole NGHP-01-08A after subtraction of the hydrostatic pressure trend. This residual pressure curve shows only minor

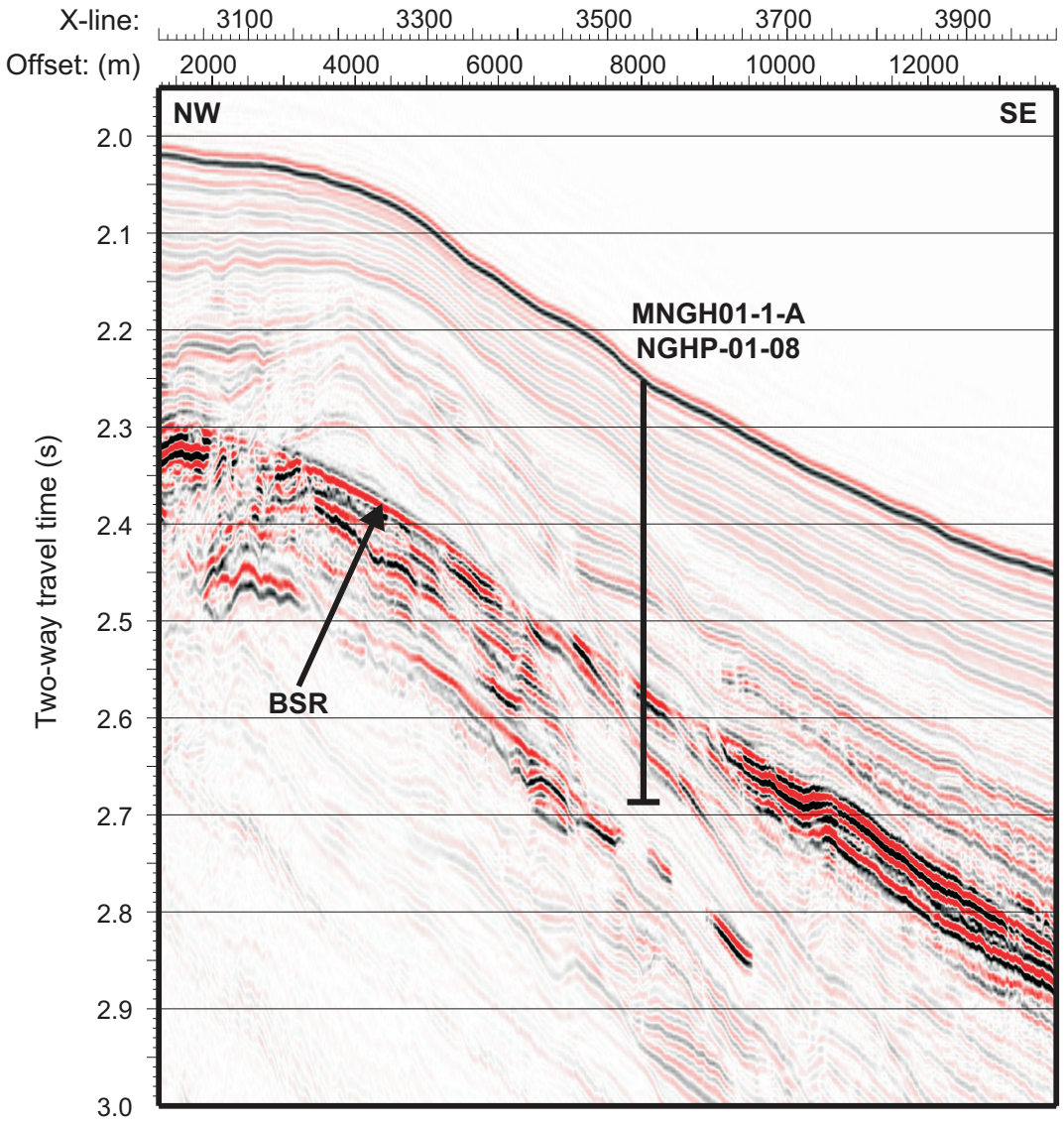

Figure 2. Section of seismic inline 2148 from 3D cube around Site NGHP-01-08 (Prospectus Site MNGH01-1-A) showing a widespread BSR associated with high-amplitude reflectors below. [BSR, bottom-simulating reflector]

fluctuations that are well below the 100 psi level that would have required preventive action. The largest pressure anomaly is a positive spike (about 50 psi) around 284 mbsf, and is most likely due to packing of cuttings in the borehole. We also monitored the coherence of the sonic waveforms acquired by the SonicVISION tool, which was configured to pick the borehole fluid wave arrival. Possible gas indicators are loss of coherence in the waveforms and a slower fluid wave velocity, which were not observed throughout the interval drilled.

LWD Log Quality

Figure 5 also shows the quality control logs for Hole NGHP-01-08A. The two curves for rate of penetration are an instantaneous rate of penetration (ROP_RM) and a rate of penetration averaged over the last 5 feet (ROP5_RM). The occasional peaks in the instantaneous rate of penetration are artifacts due to depth fluctuations during pipe connections. The ROP is generally below 30 m/h, which is sufficient to record high-resolution GeoVISION resistivity images (for details, see "Downhole Logging" in the "Methods" chapter).

The density (DCAV) and ultrasonic caliper logs (UCAV) show an enlarged hole near the seafloor (24–70 mbsf), with a hole diameter up to 12 in. The bit size (dashed line in fig. 5) is 9 7/8 in, and the ultrasonic caliper shows that most of the borehole below 100 mbsf is about 10.5 in. The density caliper, however, shows a borehole that is smaller than the bit size for most of the interval below 100 mbsf; the ultrasonic caliper is a direct measurement of borehole size and is probably more reliable. Both the density and ultrasonic caliper show a washout with a borehole diameter up to 12 in the interval 217–240 mbsf.

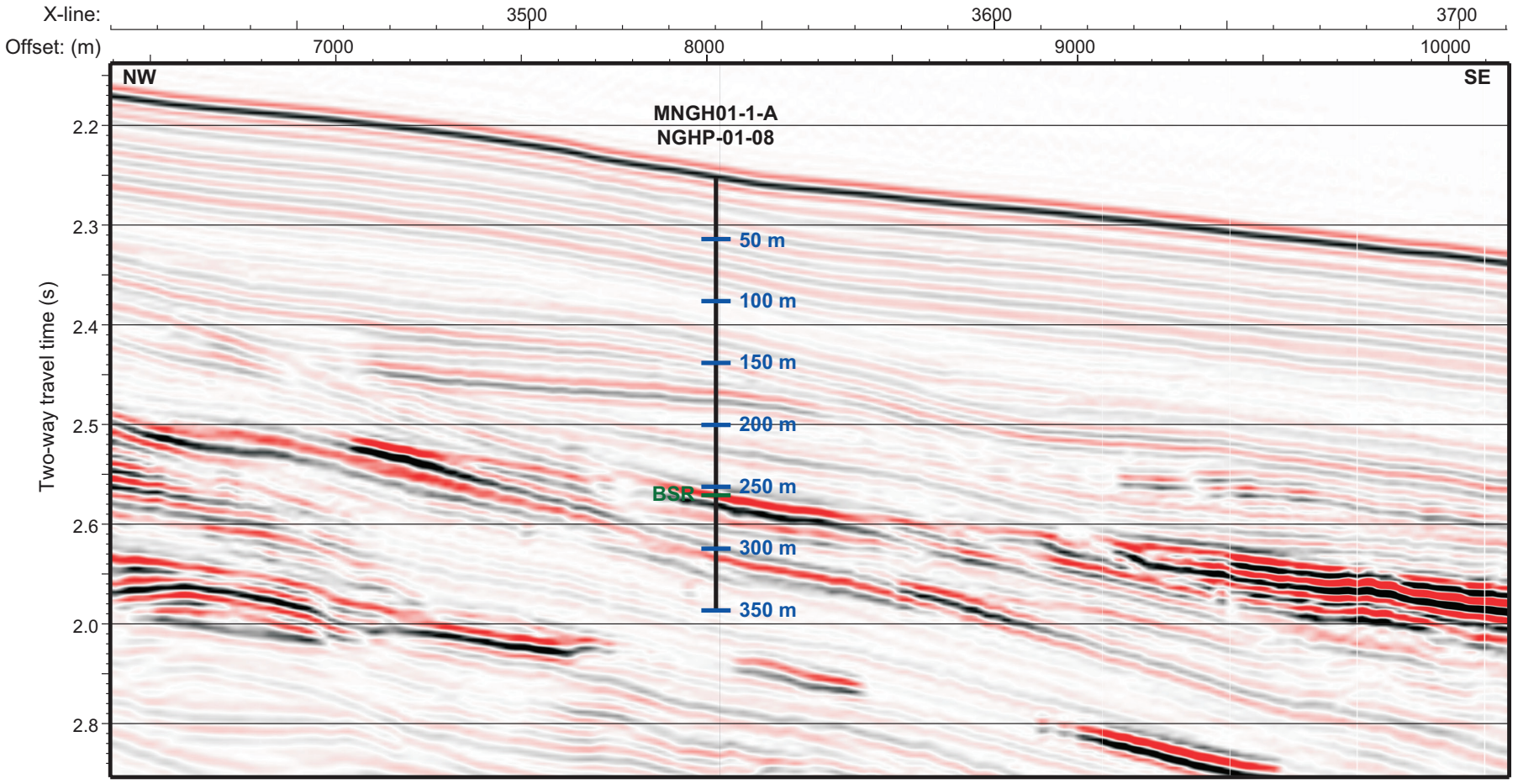

Figure 3. Close up of seismic inline 2148 around Site NGHP-01-08 (Prospectus Site MNGH01-1-A) with predicted formation tops and BSR depth (~257 mbsf) based on a uniform seismic velocity of 1,610 m/s. [BSR, bottom-simulating reflector; mbsf, meters below sea floor; m/s, meters per second]

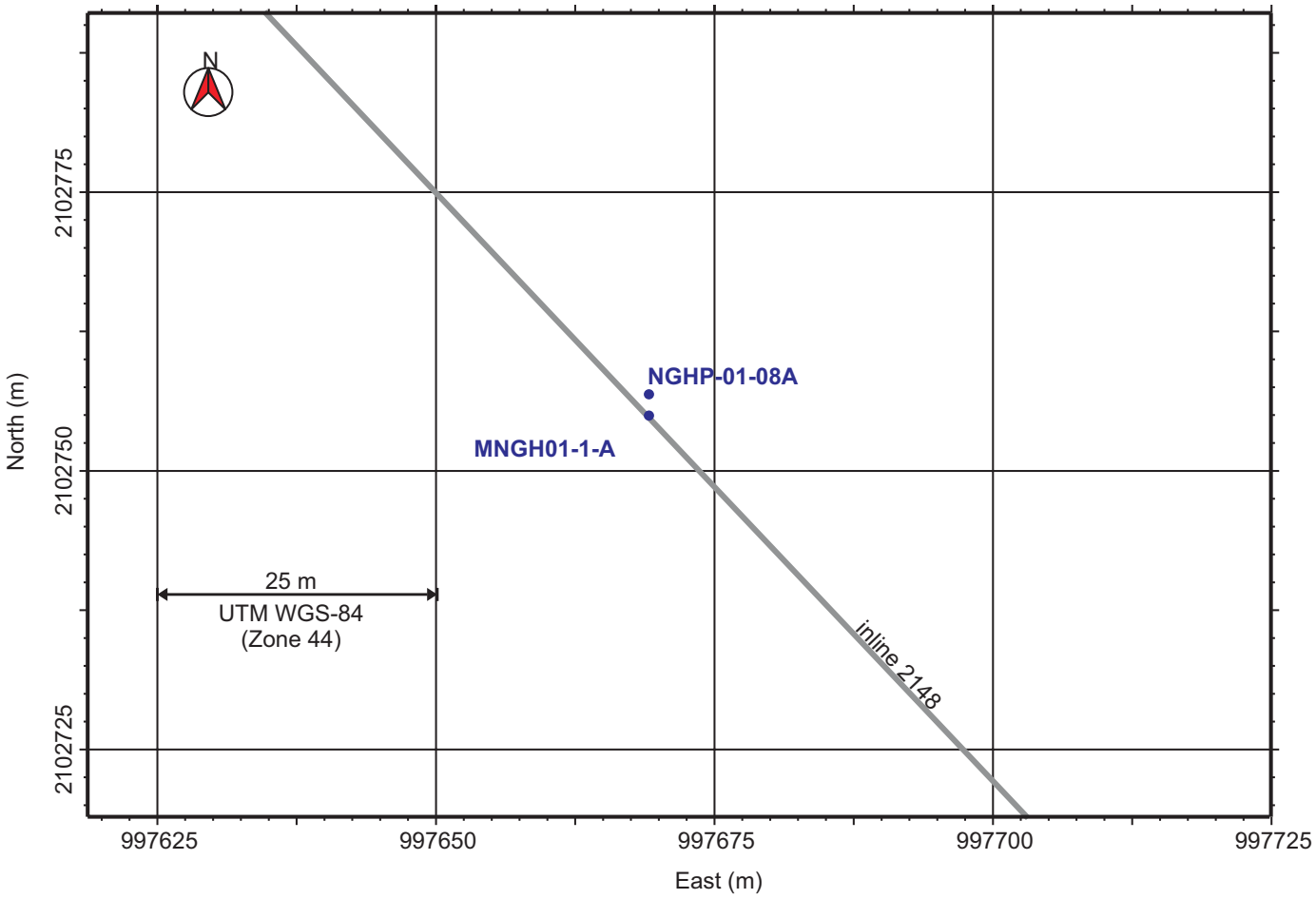

Figure 4. Map showing the hole occupied at Site NGHP-01-08 (MNGH01-1-A).

The density correction, calculated from the difference between the short- and long-spaced density measurements, is everywhere less than 0.2 g/cm^3 (fig. 5), suggesting that the density measurements should be of good quality.

Figure 6 is a summary of the LWD gamma ray, density, neutron porosity, and resistivity logs measured in Hole NGHP-01-08A. The gamma ray and resistivity logs measured by the GeoVISION and EcoScope generally agree. The GeoVISION and EcoScope gamma ray curves have the same shape, but are offset by about 20–30 gAPI; this difference is most likely due to tool calibration.

Figure 7 shows a comparison of the ring resistivity measured by the GeoVISION with the attenuation and phase resistivity curves obtained by the EcoScope tool at different frequencies and transmitter-receiver spacings. For a given transmitter-receiver spacing, the phase-shift EcoScope resistivities have higher vertical resolution than the attenuation resistivities and thus show more detail.

Figure 6 also shows two bulk density curves: RHOB is the average density obtained by the EcoScope tool while rotating, while IDRO (image-derived density) is the value of density measured when the sensors were in closest contact with the formation. The two density curves are generally close, except for a few intervals where the image-derived density is greater and likely more reliable.

The bottom-simulating reflector (BSR) that should mark the bottom of the gas-hydrate stability zone was estimated to be at a depth of 257 mbsf in this hole. The only change in the LWD logs near this depth is a small low in density and resistivity at 253 mbsf (fig. 6). The top of the borehole washout noted earlier, which may mark a poorly consolidated interval, is at 217 mbsf, shallower than the estimated BSR depth.

The depths relative to seafloor were fixed for all of the LWD logs by identifying the step change in the GeoVISION gamma ray log at the seafloor. For Hole NGHP-01-08A, the gamma ray logging pick for the seafloor was at a depth of 1,701 mbrf, 1 m deeper than the initial depth estimated by the drillers (1,700 mbrf). While a driller's tag below the seafloor detected by the LWD logs is easily explained by a soft bottom, a driller's tag above the seafloor is unexpected. This discrepancy is probably due to an imprecision in depth because the compensator cylinders may have been in a slightly different position when tagging and spudding. The rig floor logging datum was located 10.5 m above sea level.

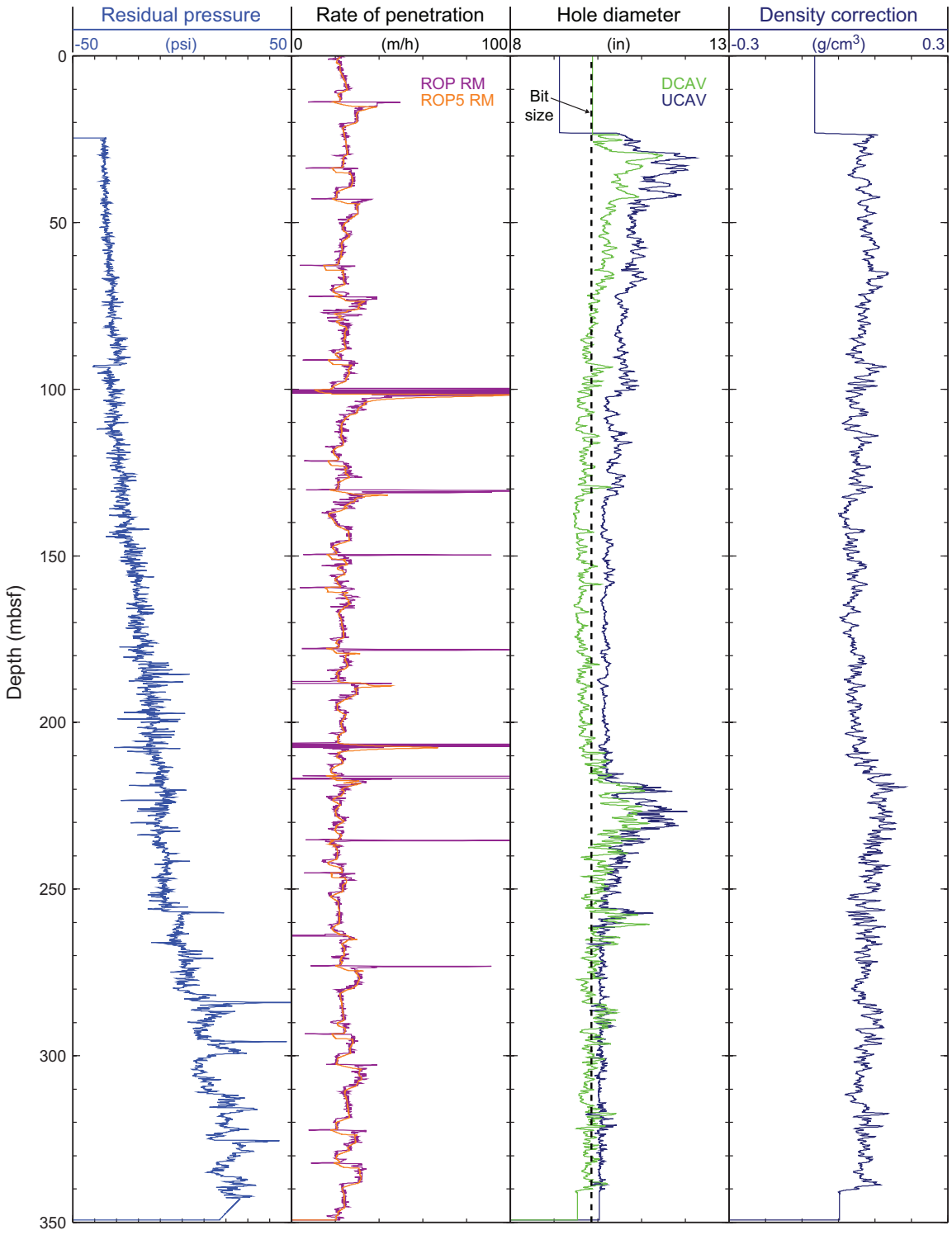

Figure 5. Monitoring and quality control LWD/MWD logs from Hole NGHP-01-08A. [LWD/MWD, logging-while-drilling/measuring-while-drilling; ROP_RM, Instantaneous rate of penetration; ROP5_RM, Rate of penetration averaged over a 5-ft interval; UCAV, Ultrasonic caliper; DCAV, density caliper.]

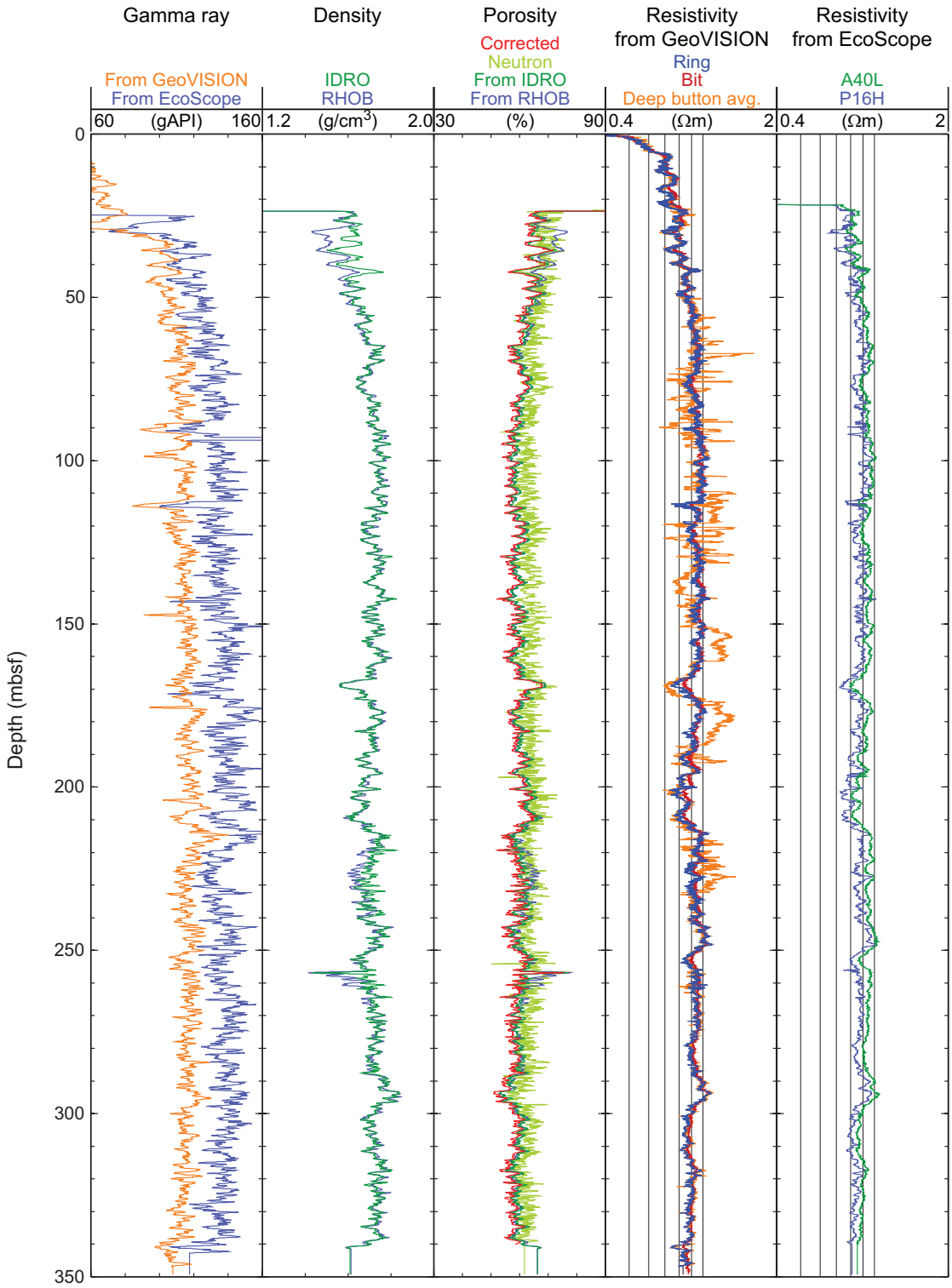

Figure 6. Summary of LWD log data from Hole NGHP-01-08A. [LWD, logging while drilling; gAPI, American Petroleum Institute gamma ray units; IDRO, Image-derived density (EcoScope); RHOB, Bulk density (EcoScope); neutron, Thermal neutron porosity (EcoScope); corrected, density porosity with core derived grain densities (EcoScope); RING, Ring resistivity (GeoVISION); BIT, Bit resistivity (GeoVISION); Deep Button avg., Button deep resistivity (GeoVISION); A40L, Attenuation resistivity measured at 400 kHz and a transmitter-receiver spacing of 40 in (EcoScope); and P16H, Phase-shift resistivity at 2 MHZ and a transmitter-receiver spacing of 16 in (EcoScope)]

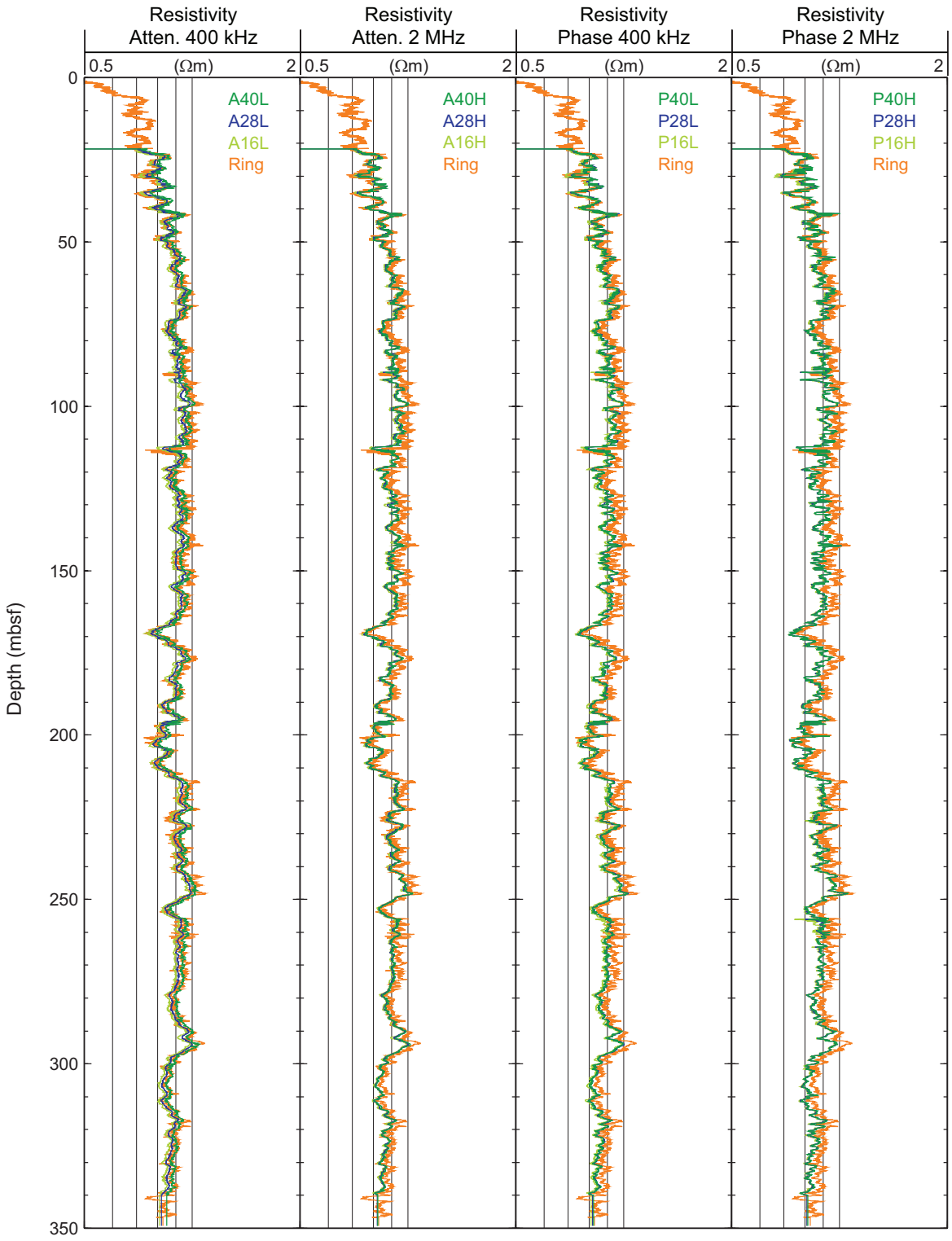

Figure 7. Comparison of LWD resistivity curves from Hole NGHP-01-08A. [LWD, logging while drilling; Ring, Ring resistivity (GeoVISION); AXXL, Attenuation resistivity measured at a frequency of 400 kHz, where XX is the transmitter-receiver spacing in inches (EcoScope); AXXH, Attenuation resistivity measured at a frequency of 2 MHz, where XX is the transmitter-receiver spacing in inches (EcoScope); PXXL, Phase-shift resistivity measured at a frequency of 400 kHz, where XX is the transmitter-receiver spacing in inches (EcoScope); PXXH, Phase-shift resistivity measured at a frequency of 2 MHz, where XX is the transmitter-receiver spacing in inches (EcoScope)]

LWD Porosities

Sediment porosities were calculated from the LWD density and neutron logs in Hole NGHP-01-08A. No core-derived physical property data were available at this site to calibrate and evaluate the log-derived porosities.

The LWD log-derived density measurements (r_b) from Hole NGHP-01-08A were used to calculate sediment porosities (φ) with the standard density-porosity relation: $\varphi = (r_g - r_b) / (r_g - r_w)$. We first used a constant water density (r_w) of 1.03 g/cm^3 and a grain/matrix density (r_g) of 2.75 g/cm^3. The density log-derived porosities from Hole NGHP-01-08A range from just above 65 percent at 23 mbsf to about 60 percent at 350 mbsf (fig. 6). The density porosities in figure 6 were calculated from both the bulk density (RHOB) and from the image-derived density (IDRO).

To estimate the influence of variable grain density, but without any core sample measurements available at this site, we calculated a "corrected porosity" from the IDRO density log and using a least square linear fit with depth of the grain density measurements made on samples from nearby Site NGHP-01-19. The results in figure 6 show only slightly lower porosity values than when assuming constant grain density.

The LWD neutron porosity log from Hole NGHP-01-08A (fig. 6) yielded sediment porosities ranging from an average value of about 70 percent at 23 mbsf to just above 60 percent at 350 mbsf. Porosities measured by the neutron log are expected to be higher than those computed from the density log in clay-rich sediments, because the neutron log essentially quantifies hydrogen abundance, and counts hydrogen in clay minerals as porosity. The neutron porosity measured by the EcoScope tool shown in figure 6 is the "best thermal neutron porosity" (BPHI); it has been corrected for density so that the effect of clay is reduced (Adolph and others, 2005), and it is only marginally higher than the density porosity.

LWD Borehole Images

The GeoVISION and EcoScope LWD tools generate high-resolution images of borehole log data. The EcoScope tool produces images of density and hole radius (computed on the basis of the density correction, which depends on the borehole standoff). The GeoVISION produces a gamma ray image and resistivity images with shallow, medium and deep depth of investigation.

Figure 8 shows some of the LWD images collected by the EcoScope and GeoVISION tools. It should be noted that the display in figure 8 is highly compressed in the vertical direction. The unwrapped images are about 80 cm wide (for a 10 in diameter borehole) and the vertical scale is compressed relative to the horizontal by a factor of about 55:1. These high-resolution images can be used for detailed sedimentological and structural interpretations and to image gas-hydrate distribution in sediments (for example, in layers, nodules, fractures). Gas-hydrate-bearing sediments exhibit high resistivities within intervals of uniform or low bulk density. Layers with high resistivity and high density are likely to be low porosity, compacted, or carbonate-rich sediments. The two resistivity images in figure 8 correspond to two depths of investigation (for details, see "Downhole Logging" in the "Methods" chapter).

Gas-hydrate-rich intervals show up in the LWD images as high resistivity intervals that do not correspond to matching high densities. There is no indication of the presence of gas hydrate in the LWD images in figure 8.

Gas-Hydrate and Free Gas Occurrence

As previously discussed (see "Downhole Logging" in the "Methods" chapter), the presence of gas hydrate is generally identified by increases in electrical resistivity and acoustic velocity that are not accompanied by a corresponding porosity decrease. A decrease in porosity alone in water-saturated sediments can result in an increase in resistivity and acoustic velocity. Resistivity logs in Hole NGHP-01-08A show a general negative correlation with porosity (fig. 6), suggesting that little or no gas hydrate is present.

To make a quantitative estimate of the amount of gas hydrate at Site NGHP-01-08, we followed the procedure described in "Downhole Logging" in the "Methods" chapter, to apply the Archie relationship to the resistivity and porosity logs recorded in Hole NGHP-01-08A.

The procedure and the results are shown in figure 9. The pore fluid resistivity (R_w) was estimated from Fofonoff (1985) using a linear temperature profile derived from the *in situ* temperature measurements at nearby Site NGHP-01-19 (4.78 °C at the seafloor; gradient of 52.3 °C/km; see "Physical Properties" in the "Site NGHP-01-19" chapter) and a water salinity defined by the least square power law fit with depth of the values measured on pore water samples from Site NGHP-01-19. The estimated m curve is derived from R_w, the porosity (φ) and resistivity (R_t) logs ($m_{est} = -\log F/\log\varphi$, where $F = R_t / R_w$). As this relationship is defined for water-saturated sediments, the chosen value of $m = 2.2$ is given by the baseline of this curve in the low-resistivity intervals where there is likely no gas hydrate. Using the porosity log and Archie's equation ($R_0 = (a\, R_w) / f^m$), we derive the predicted resistivity

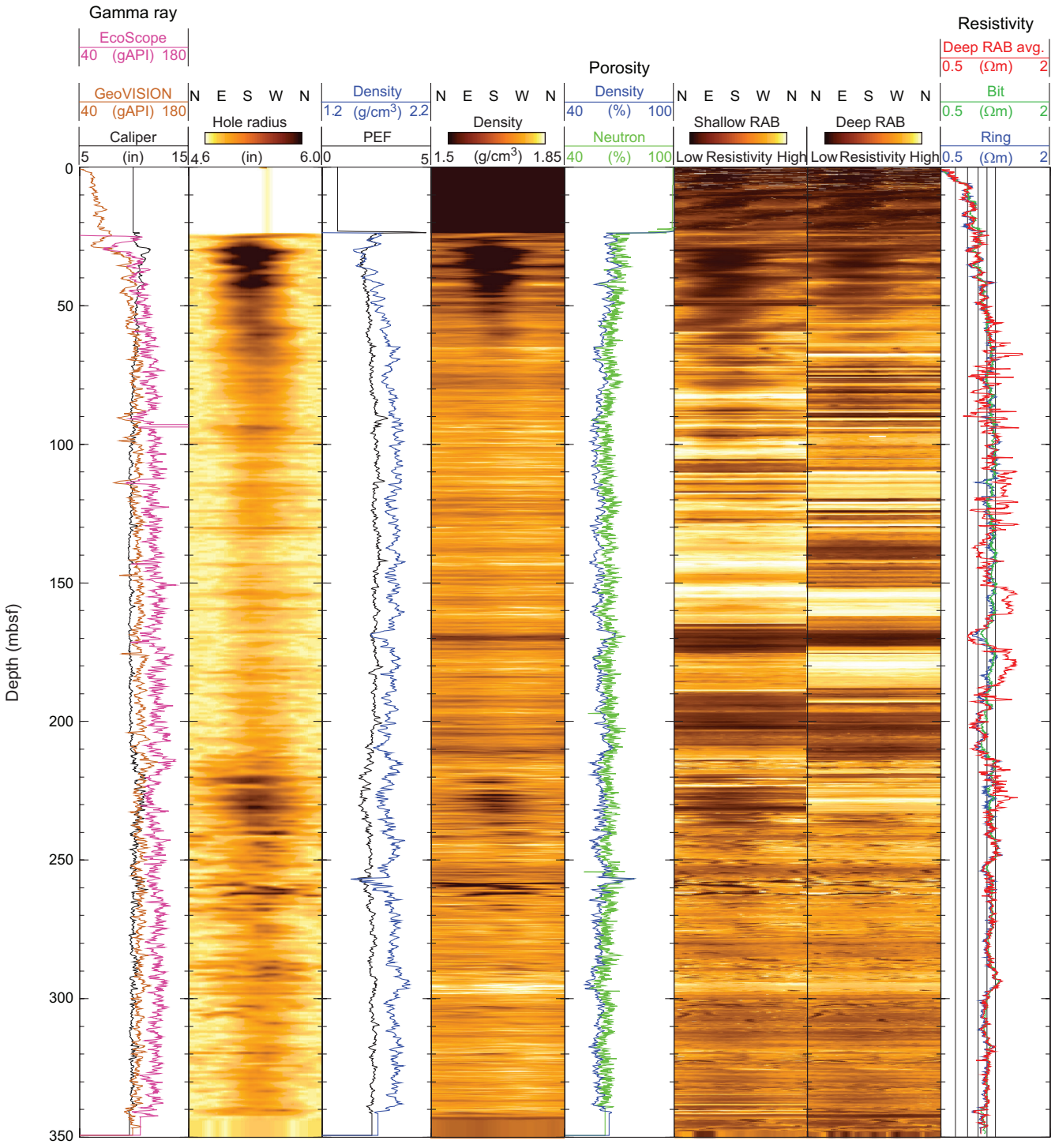

Figure 8. LWD image data from Hole NGHP-01-08A. [LWD, logging while drilling; gAPI, American Petroleum Institute gamma ray units; RAB, Resistivity-At-Bit image obtained by the GeoVISION tool]

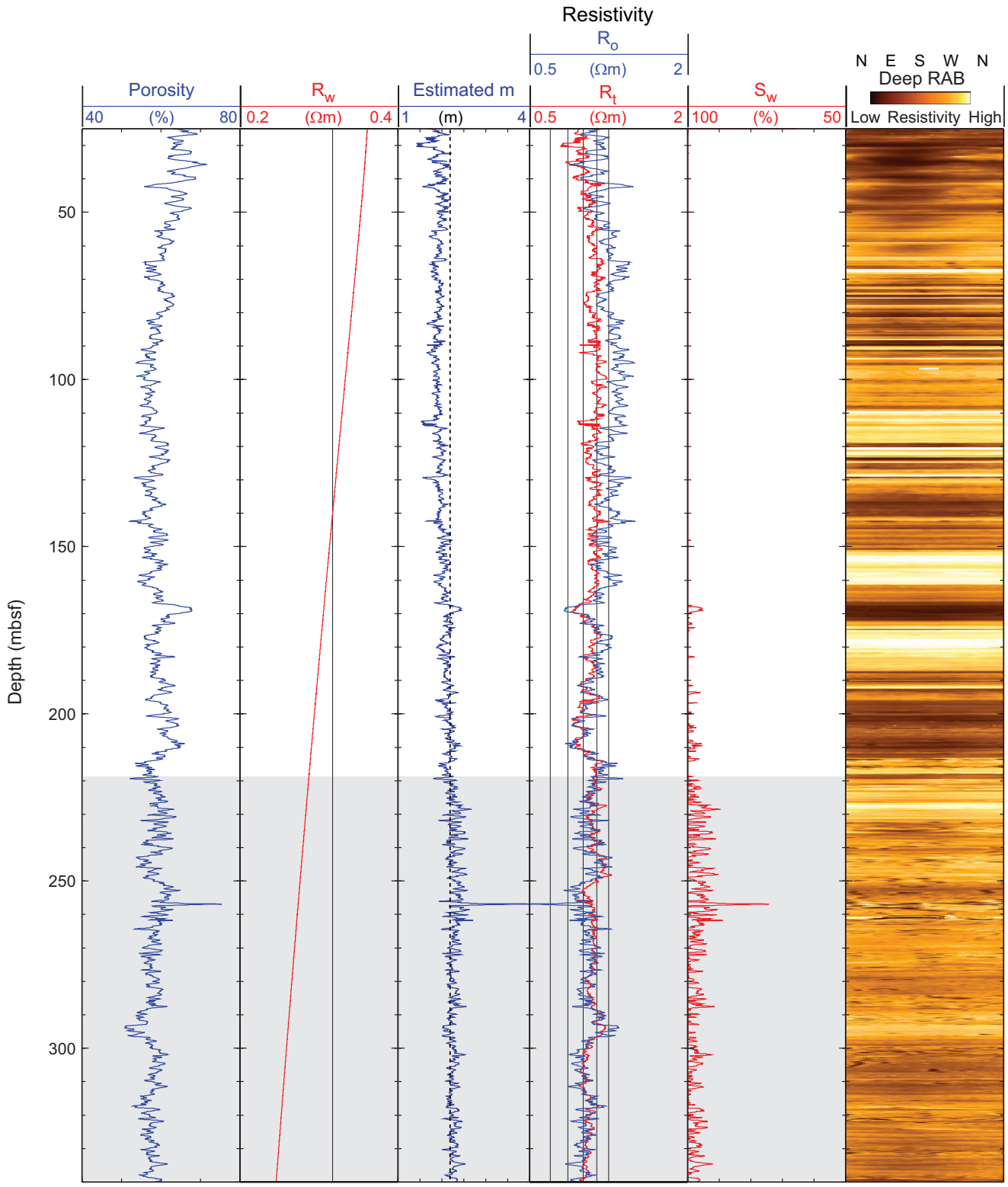

Figure 9. Water saturations from Archie's equation and LWD porosity and resistivity logs in Hole NGHP-01-08A. The gray area indicates degraded data quality. [LWD, logging while drilling; Rw, Formation water resistivity; R0, Computed formation resistivity for 100 percent water saturation; Rt, Measured resistivity; Sw, water saturation]

of the water-saturated formation R_o. A qualitative influence of gas hydrate on the resistivity log is indicated by the difference between the R_0 and the measured resistivity R_t. The estimated water saturation, assumed to be the numerical complement of the hydrate saturation, is $S_w = (R_0/R_t)^{1/n}$, where n=2 (Pearson and others, 1983). We used the "corrected" density porosity computed from the image-derived density (IDRO) and the resistivity from the 16 in, phase-shift, high-frequency propagation resistivity (P16H) measured by the EcoScope tool. We use the P16H curve because it is the resistivity with the highest vertical resolution measured by the EcoScope.

As noted earlier, the porosity and resistivity curves in Hole NGHP-01-08A generally mirror each other, so that the computed water-saturated resistivity R_0 is very close to the measured resistivity R_t and the water saturation S_w is close to 100 percent above ~220 mbsf (fig. 9). Below this depth, the results suggest that as much as 10 percent of the pore space could be occupied either by gas hydrate above the BSR (estimated at ~257 mbsf, see "Background and Objectives") or by free gas below.

References Cited

Adolph, B., Archer, M., Codazzi, D., el-Halawani, T., Perciot, P., Weller, G., Evans, M., Grant, J., Griffiths, R., Hartman, D., Sirkin, G., Ichikawa, M., Scott, G., Tribe, I., and White, D., 2005, No more waiting—Formation evaluation while drilling: Oilfield Review, Autumn 2005, p. 4–21.

Aldred, W., Cook, J., Bern, P., Carpenter, B., Hutchinson, M., Lovell, J., Rezmer-Cooper, I., and Leder, P.C., 1998, Using downhole annular pressure measurements to improve drilling performance: Oilfield Review, Winter 1998, p. 40–55.

Fofonoff, N.P., 1985, Physical properties of seawater: Journal of Geophysical Research, v. 90, no. C2, p. 3332–3342.

Pearson, C.F., Halleck, P.M., McGuire, P.L., Hermes, R., and Mathews, M., 1983, Natural gas hydrate deposits—A review of *in situ* properties: Journal of Physical Chemistry, v. 87, p. 4180–4185.